REPORT DOCUMENTATION PAGE

AFRL-SR-AR-TR-05-

0518

1. AGENCY USE ONLY *(Leave blank)*	2. REPORT DATE	3. REPOR... AND DATES COVERED
		01 Jul 2002 - 30 Jun 2005 FINAL

4. TITLE AND SUBTITLE
PLASMONIC DEVICES AND MATERIALS

5. FUNDING NUMBERS
61102F
2305/DX

6. AUTHOR(S)
DR ATWATER

7. PERFORMING ORGANIZATION NAME(S) AND ADDRESS(ES)
CALIFORNIA INSTITUTE OF TECHNOLOGY
1201 E CALIFORNIA BLVD MAIL CODE 202-6
PASADENA CA 91125

8. PERFORMING ORGANIZATION REPORT NUMBER

9. SPONSORING/MONITORING AGENCY NAME(S) AND ADDRESS(ES)
AFOSR/NE
4015 WILSON BLVD
SUITE 713
ARLINGTON VA 22203

10. SPONSORING/MONITORING AGENCY REPORT NUMBER
F49620-02-1-0324

11. SUPPLEMENTARY NOTES

12a. DISTRIBUTION AVAILABILITY STATEMENT
DISTRIBUTION STATEMENT A: Unlimited

12b. DISTRIBUTION CODE

13. ABSTRACT *(Maximum 200 words)*

This final technical report reviews our scientific and technical development in the area of new plasmonic devices and materials undertaken during our AFOSR support from July 2002-June 2005. This report contains a summary overview of scientific and technical progress and results over the entire program. It also provides detail about recent technical conducted during Period 3 of the present grant. Our work since the inception of the program has focused on development of materials and electromagnetic designs plasmonic devices at the subwavelength-to-wavelength scale. The effort includes experimental research on use of near field interactions to enable optical guiding and switching below the diffraction limit and is complemented by theoretical work on near field interactions in and collective modes of subwavelength scale metallodielectric structures.

14. SUBJECT TERMS			15. NUMBER OF PAGES / 16. PRICE CODE
17. SECURITY CLASSIFICATION OF REPORT	**18. SECURITY CLASSIFICATION OF THIS PAGE**	**19. SECURITY CLASSIFICATION OF ABSTRACT**	**20. LIMITATION OF ABSTRACT**
Unclassified	Unclassified	Unclassified	UL

Status of Effort:

This final technical report reviews our scientific and technical development in the area of new plasmonic devices and materials undertaken during our AFOSR support from July 2002-June 2005. This report contains a summary overview of scientific and technical progress and results over the entire program. It also provides detail about recent technical conducted during Period 3 of the present grant. Our work since the inception of the program has focused on development of materials and electromagnetic designs plasmonic devices at the subwavelength-to-wavelength scale. The effort includes experimental research on use of near field interactions to enable optical guiding and switching below the diffraction limit and is complemented by theoretical work on near field interactions in and collective modes of subwavelength scale metallodielectric structures.

Scientific and Technical Highlights:

Highlights over the three year grant include

- First experimental and theoretical demonstration of **light guiding below the diffraction limit in nanoparticle plasmon waveguides**,
- Experimental and theoretical demonstration of resonant **plasmon printing of 40 nm lithographic features in conventional AZ photoresist** using visible (410 nm) light.
- Theoretical demonstration of enhanced subwavelength near field optical resolution by use of a 30 nm Ag film as a lens.
- Theoretical investigation of **optical pulse propagation** in subwavelength scale **plasmon waveguides**,
- Experimental and theoretical demonstration of strongly coupled nanoparticle chain arrays in the 'sub-lithographic' size regime, i.e, particle size of ~10 nm and interparticle separations of 1-4 nm.
- Defined limits for enhanced subwavelength image resolution in negative permittivity materials , applied to near field optical resolution in thin Ag films. .

By way of enumeration, the following outputs from the grant are noted:

- 41 invited presentations in international conferences and workshops and university/laboratory seminar series.
- 25 publications with full or partial AFOSR including a recent review paper.
- *One paper[1] has already been cited over 100 times and is among the top ten cited papers in Nature Materials since that journal's inception in 2002.* .
- Two papers[1,2] have been featured as cover articles for Nature Materials.

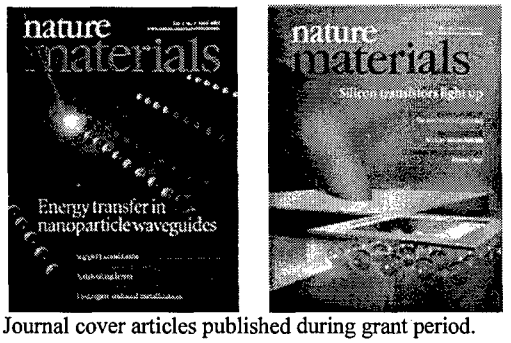

Journal cover articles published during grant period.

Ongoing efforts include studies of in-coupling and out-coupling efficiency from plasmon waveguides into free space modes and coupling into subwavelength scale plasmonic nanoparticles and hole-array structures, as well as efforts to develop tunable plasmonic materials by incorporating thin film electrooptic materials and photoaddressable polymers into plasmonic materials and devices.

---

[1] **"Local detection of electromagnetic energy transport below the diffraction limit in metal nanoparticle plasmon waveguides"**, Stefan A. Maier, Pieter G. Kik, Harry A. Atwater, Sheffer Meltzer, Elad Harel, Bruce E. Koel and Ari A.G. Requicha, Nature Materials, **2**, 232 (2003).

[2] **"Field-effect electroluminescence in silicon nanocrystals"**, R.J. Walters, G.I. Bourianoff, H.A. Atwater HA Nature Materials **4** (2): 143-146 FEB 2005

Recent Accomplishments/New Findings:

MIM Plasmon Slot Waveguides

We have recently performed a numerical analysis of *metal/insulator/metal (MIM) surface plasmon 'slot' waveguides which are seen to exhibit both long-range propagation and spatial confinement of light with lateral dimensions of less than 10 percent of the free-space wavelength* in two-dimensional $Ag/SiO_2/Ag$ structures with waveguide thicknesses ranging from 12nm to 0.25μm. As in conventional planar insulator/metal/insulator (IMI) thin film surface plasmon waveguides, analytic dispersion results indicate a splitting of plasmon modes – corresponding to symmetric and antisymmetric electric field distributions – as SiO_2 core thickness is decreased below 100nm. From visible to near infrared wavelengths, plasmon propagation exceeds tens of microns with fields confined to within 20 nanometers of the structure. As the SiO_2 core thickness is increased, propagation distances also increase with localization remaining constant.

When a plasmon is excited at a metallodielectric interface, electrons in the metal create a surface polarization that gives rise to a localized electric field. In IMI structures, electrons of the metallic core screen the charge configuration at each interface and maintain a near-zero (or minimal) field within the waveguide. As a result, the surface polarizations on either side of the metal film remain in phase and a cutoff frequency is not observed for any transverse waveguide dimension. In contrast, screening does not occur within the dielectric core of MIM waveguides. At each metal/dielectric interface, surface polarizations arise and evolve independently of the other interface, and plasma oscillations need not be energy or wavevector-matched to each other. Therefore, for certain MIM dielectric core thicknesses, interface SPs may not remain in phase but will exhibit a beating frequency; as transverse core dimensions are increased, "bands" of allowed energies/wavevectors and "gaps" of forbidden energies will be observed.

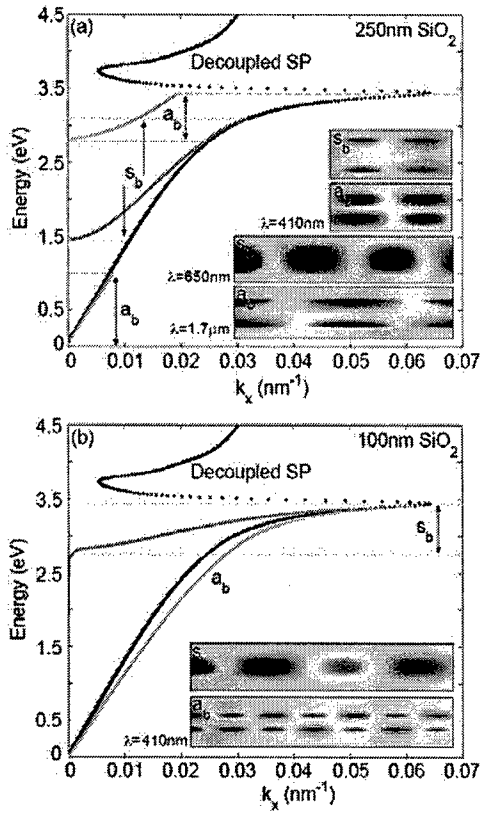

Figure 1: Dispersion relations for MIM planar waveguides with a SiO_2 core and an Ag cladding. (a) For oxide thicknesses of 250nm, the structure supports conventional waveguiding modes with cutoff wavevectors observed for both the symmetric (s_b, dark gray) and antisymmetric (a_b, light gray) field configurations. (b) As oxide thickness is reduced to 100nm, both conventional and plasmon waveguiding modes are supported. Accordingly, tangential electric fields are localized within the core for conventional modes but propagate along the metal/dielectric interface for plasmon modes, (inset, plotted in (a) at free-space wavelengths of λ=410nm (~3eV) (top two panels), λ=650nm (~1.2eV), and λ=1.7μm (~0.73eV), and in (b) at λ=410nm (~3eV)).

This behavior is illustrated in Fig. 1, which plots the dispersion relations for an MIM waveguide with core thicknesses of 250nm (Fig. 1a) and 100nm (Fig. 1b). The waveguide consists of a three-layer metallodielectric stack with an SiO_2 core and an Ag cladding. The metal is defined by empirical optical constants. Allowed wavevectors are seen to exist for all free space wavelengths (energies) and exhibit exact agreement with the dispersion relation for a single Ag/SiO_2 interface SP. Figure 1a plots the bound modes (i.e, modes occurring at frequencies below the SP resonance) of an $Ag/SiO_2/Ag$ waveguide with core thickness d=250nm. As seen, multiple bands of allowed and forbidden frequencies are observed. The allowed a_b modes follow the light line for energies below ~1eV and resemble conventional dielectric core/ *conducting* cladding waveguide modes for energies above ~2.8eV. Tangential electric fields in each a_b regime (considering free-space wavelengths of λ=410nm (~3eV) and λ=1.7μm (~0.73eV)) are plotted in the inset and illustrate the photonic and transverse electric nature, respectively, of the modes. In contrast, the s_b modes are only observed for energies between 1.5 and 3.2eV. Dispersion for this mode is reminiscent of conventional dielectric core/ *dielectric* cladding waveguides, with endpoint asymptotes corresponding to tangent line slopes (effective indices) of n=8.33 at 1.5eV and n=4.29 at 3.2eV. For energies exceeding ~2.8eV, wavevectors of the s_b mode are matched with those of the SP, and the tangential electric field transits from a core mode to an interface mode (see the top (1st) and 3rd panels of the inset, comparing

λ=410nm (~3eV) and λ=650nm (~1.9eV)). As the core layer thickness is increased through 1μm (data not shown), the number of a_b and s_b bands increases with the a_b modes generally lying at higher energies. In analogy with conventional waveguides, larger (but bounded) core dimensions increase the number of modes supported by the structure.

Figure 1b plots the bound mode dispersion curves for an MIM waveguide with SiO_2 core thickness d=100nm. *Although the s_b mode resembles conventional waveguide dispersion, the a_b mode is seen to exhibit plasmon-like behavior.* The inset shows snapshots of the tangential electric field for both modes at a free-space wavelength λ=410nm (~3eV). *The presence of both of conventional and SP waveguiding modes represents a transition to subwavelength-scale photonics.*

Figure 2 illustrates this interdependence of skin depth and propagation in MIM structures for film thickness from 12nm-250nm. The top panels plot propagation for the structure as a function of free space wavelength; the bottom panels plot the corresponding skin depth. Figure 2a plots propagation and skin depth for a 250nm oxide layer. The symmetric bound mode is seen to propagate for wavelengths between 400 and 850nm, with maximum propagation distances of ~15μm. *In contrast, the antisymmetric bound mode is seen to propagate distances of 80μm for wavelengths greater than 1250nm.* In regions of high propagation (i.e., above 1250nm), skin depth remains approximately constant at 20nm.

Figure 2b illustrates the propagation distance and skin depth for the asymmetric bound mode for oxide thicknesses from 12nm-100nm. The continuous plasmon-like dispersion relations of Fig. 1b is well correlated with the observed propagation: decay lengths are longest for larger wavelengths, where dispersion follows the light line. Plasmon propagation generally increases with increasing film thickness, approaching ~10μm for a 12nm oxide layer and ~40μm for a 100nm thick oxide. Nevertheless, field penetration remains approximately constant in the Ag cladding, never exceeding 20nm. Thus, unlike conventional plasmon waveguides, MIM waveguides can achieve micron-scale propagation with nanometer-scale confinement.

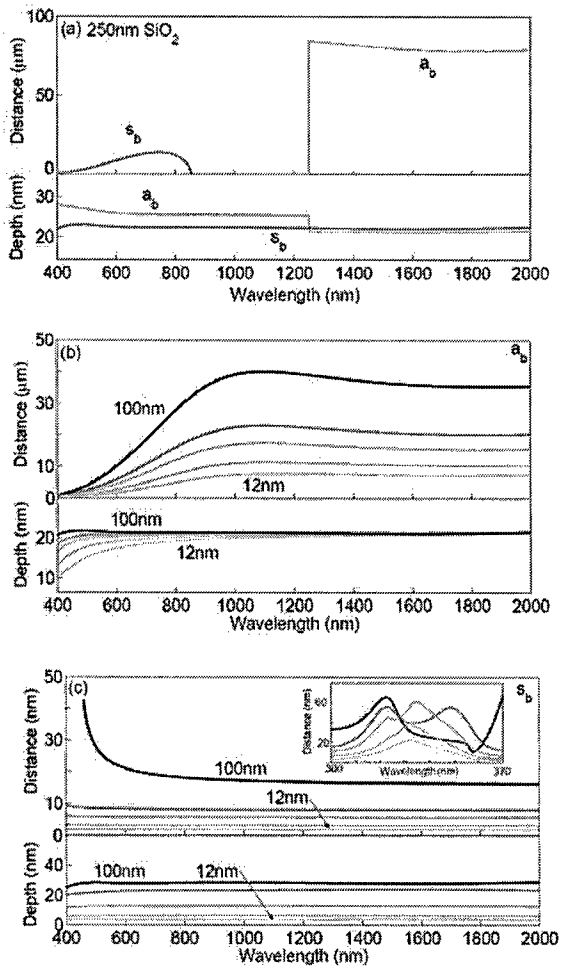

Figure 2: MIM ($Ag/SiO_2/Ag$) propagation and skin depth plotted as a function of wavelength for core thicknesses of d=250nm (a) and d=12nm, 20nm, 35nm, 50nm, and 100nm (b, c). In panel (a), propagation lengths of conventional (as opposed to plasmonic) waveguiding modes are recovered and correlated with skin depth. In (b), the field antisymmetric modes of MIM guides are seen to propagate over 10 microns with skin depth never exceeding 20nm. In (c), the symmetric modes of thinner films (d≤50nm) remain evanescent for all wavelengths. However, as *d* approaches 100nm, conventional waveguiding modes can be accessed, and a region of enhanced propagation is observed for λ≤400nm. Inset: Propagation distances of the symmetric mode for wavelengths characteristic of the quasi-bound regime. The dissociation of the thin-film single peak to the thick-film double peak indicates the onset of conventional waveguiding.

Plasmon-Enhanced Emission from Silicon Nanocrystals

We have investigated the local-field-enhanced light emission from silicon nanocrystals close to a film of nanostructured (nanoporous) gold (Fig. 3). The *luminescence intensity enhancement results from increases in coupled silicon nanocrystal/nanoporous gold absorbance cross section, radiative decay rate and quantum efficiency*. We resolve photoluminescence as the gold-Si nanocrystal separation distance is varied between 0 and 20 nm, and observe an up to 8-fold luminescence intensity enhancement dependent on pump power and

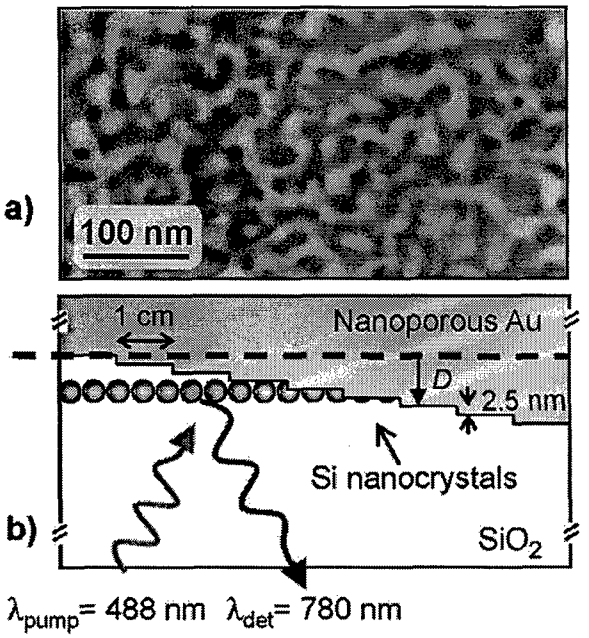

Figure 3 - a) False color plan view (100k magnification) SEM of the nanoporous gold surface showing features on the order of 10 nm. b) Schematic cross section of the sample. PL measurements are made from the bottom side of all samples.

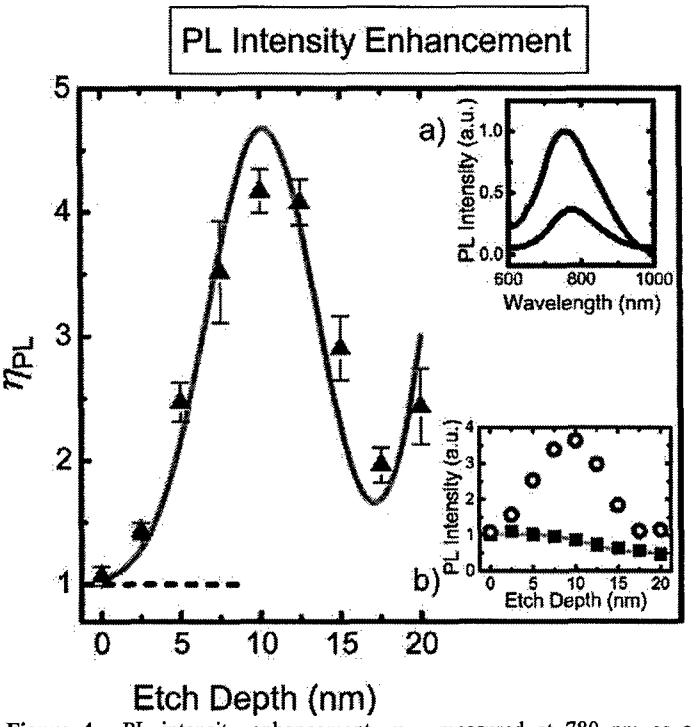

Figure 4. PL intensity enhancement, η_{PL}, measured at 780 nm as a function of etch depth, D (triangles). The solid line is a fit to the data using a model that accounts for the spatial distribution of Si nanocrystals and the enhanced local-field. Insets: a) Typical PL spectra for the reference (black) and coupled np-Au/nc-Si (red) samples, at D = 5 nm. b) PL intensities at 780 nm vs. etch depth for the reference (squares) and coupled np-Au/nc-Si (circles) samples. The reference intensities are well fit by the green line, which is the integral of two Gaussian distributions that peak at 14.2 nm and 24.2 nm, respectively.

separation distance. Emission in the 760 – 800 nm range indicates the radiative decay rate is enhanced more than 4-fold (to 57.5 kHz), the absorbance cross section is more than doubled (to 3.1×10^{-16} cm^2), and the quantum efficiency is enhanced more than 2-fold (to 58%). The optimal silicon nanocrystal/nanoporous gold spacing is found to be 1.6 nm, with local-field enhanced emission dominating at intermediate distances, on and off the plasmon resonance, while luminescence-quenching processes dominate at small gold-nanocrystal separations.

Typical PL spectra from the reference and np-Au/nc-Si samples are reported in inset a) of Figure 4 (black and red lines, respectively) for an etch depth, D = 5 nm, and for an excitation power density, P_{ex} = 50 mW/mm^2. The PL intensity of the coupled sample is enhanced and slightly blue-shifted with respect to the reference sample. To understand better the origin of this PL enhancement we fixed the detection wavelength at 780 nm, thus focusing our investigation only on a precise Si nanocrystal size as nc-Si PL is size-

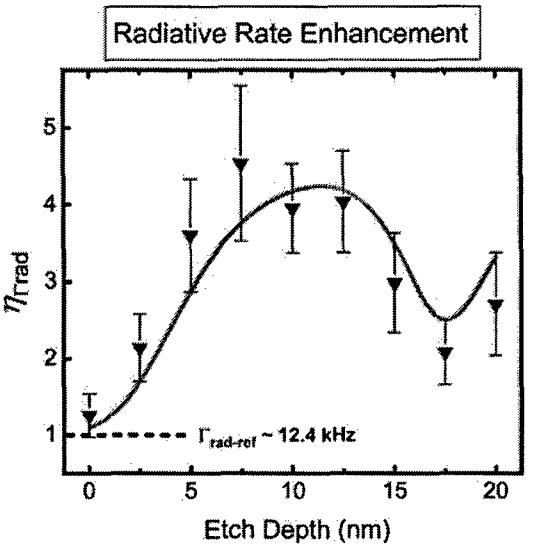

Figure 5. Radiative decay rate enhancement, η_{Trad}, calculated with eq 3 for nc-Si emitting at 780 nm coupled to the np-Au film. The solid line is a fit to the data using a model that accounts for the spatial distribution of Si nanocrystals and the enhanced local-field.

dependent. In inset b) of Figure 4, the PL intensities measured at 780 nm for both the reference (squares) and the np-Au/nc-Si coupled sample (circles) are reported as a function of D.

We also were able to measure the plasmon-enhancement factor for Si nanocrystal radiative emission. Wemeasured the experimental decay rate Γ_{exp} at P_{ex} = 50 mW/mm^2, and together with the measured enhancement in photoluminescence intensity η_{PL}, shown in Figures 5, we can directly estimate the increase in nanocrystal radiative rate $\eta_{\Gamma rad}$ for the nc-Si emitting at 780 ± 20 nm. The results are the inverted triangles in Figure 5. The enhancement $\eta_{\Gamma rad}$ depends strongly on nc-Si/nanoporous Au separation D, in particular it is greater than unity at all separation distances with a peak of ~4.5 at D = 7.5 nm. Indeed, this value suggests that *the plasmon-enhanced nanocrystal radiative decay rate* reported in Figure 5 *is uniquely responsible for the observed enhancement in PL intensity* in Figure 4.

Personnel Supported:

Faculty: Dr. Harry A. Atwater
Postdocs:
Graduate Students: Luke A. Sweatlock, Jennifer A. Dionne (partial), Robert Walters, Julie Biteen
Visiting Faculty: Dr. Albert Polman (partial)

Publications: Peer-reviewed publications submitted and/or accepted during the 12-month period starting the previous 1 October (or since start for new awards).

Period 1:

1. **"Observation of coupled plasmon-polariton modes in Au nanoparticle chain waveguides of different lengths: Estimation of waveguide loss"** Stefan A. Maier, Pieter G. Kik, and Harry A. Atwater, Appl. Phys. Lett., **81**, 1714 (2002).

2. **"Observation of coupled plasmon-polariton modes of plasmon waveguides for electromagnetic energy transport below the diffraction limit"**
   Stefan A. Maier, Pieter G. Kik, Harry A. Atwater, Sheffer Meltzer, Ari A.G. Requicha, and Bruce E. Koel, Proceedings of SPIE 4810 (2002)

3. **"Metal nanoparticle arrays for near field optical lithography"**
   Pieter G. Kik, Andrea L. Martin, Stefan A. Maier, and Harry A. Atwater, Proceedings of SPIE 4810 (2002).

4. **"Observation of near-field coupling in metal nanoparticle chains using far-field polarization spectroscopy"** Stefan A. Maier, Mark L. Brongersma, Pieter G. Kik, and Harry A. Atwater Physical Review B **65**, 193408 (2002).

5. **"Observation of coupled plasmon-polariton modes of plasmon waveguides for electromagnetic energy transport below the diffraction limit"**
   Stefan A. Maier, Pieter G. Kik, Mark L. Brongersma, Harry A. Atwater, Sheffer Meltzer, Ari A.G. Requicha, and Bruce E. Koel, MRS Proceedings 722, L6.2 (2002).

6. **"Plasmon Printing - a new approach to near-field lithography"** Pieter G. Kik, Stefan A. Maier, and Harry A. Atwater, MRS Proceedings 705 Y3.6 (2002).

7. **"Electromagnetic Energy Transport Along Yagi Arrays"**, Maier SA, Brongersma ML, Atwater HA Materials Science & Engineering C-Biomimetic and Supramolecular Systems **19**: 291-294 (2002).

8. "**Guiding Light**" Harry A. Atwater, OE Magazine (SPIE), pp 42-44, July 2002

9. **"Local detection of electromagnetic energy transport below the diffraction limit in metal nanoparticle plasmon waveguides"**, Stefan A. Maier, Pieter G. Kik, Harry A. Atwater, Sheffer Meltzer, Elad Harel, Bruce E. Koel and Ari A.G. Requicha, Nature Materials, **2**, 232 (2003).

Period 2:

10. "**Optical pulse propagation in metal nanoparticle chain waveguides**" S. A.Maier, P.G. Kik, H.A. Atwater Physical Review B **67** (20): Art. No. 205402 MAY 15 (2003)

11. "**Mega-electron-volt ion beam induced anisotropic plasmon resonance of silver nanocrystals in glass**" J.J. Penninkhof, A. Polman, L.A. Sweatlock, S.A. Maier, H.A. Atwater, A.M. Vredenberg, B.J. Kooi Appl. Phys. Lett **83** (20): 4137-4139 (2003)

12. **"Nanocrystal research targets optoelectronic components"** Walters RJ, Biteen JS, Bourianoff GI, Atwater HA Laser Focus World **40** (9): 77-80 (2004)

13. **"Silicon optical nanocrystal memory"** Walters RJ, Kik PG, Casperson JD, **Atwater HA**, Lindstedt R, Giorgi M, Bourianoff G, APPLIED PHYSICS LETTERS **85** (13): 2622-2624 (2004)

14. **"Large spectral birefringence in photoaddressable polymer films"**,B.L. Lachut, S.A. Maier, H.A. Atwater, M.J.A. de Dood, Polman A, Hagen R, Kostromine S ADVANCED MATERIALS **16** (19): 1746 (2004).

15. "**Image resolution of surface-plasmon-mediated near-field focusing with planar metal films in three dimensions using finite-linewidth dipole sources**" Kik PG, Maier SA, Atwater HA Physical Review B **69** (4): Art. No. 045418 (2004)

Period 3:

16. **"Plasmonics: Localization and guiding of electromagnetic energy in metal/dielectric structures"**, S.A. Maier, H,A Atwater J. Appl. Phys. **98** (1): Art. No. 011101 (2005)

17. "**Quenching of Si nanocrystal photoluminescence by doping with gold or phosphorous"**, A.L.Tchebotareva, M.J.A.de Dood, J.S.Biteen, H.A.Atwater, A. Polman, J. Luminescence **114** (2): 137-144 (2005)

18. **"Highly confined electromagnetic fields in arrays of strongly coupled Ag nanoparticles"**, L.A. Sweatlock, S.A. Maier, H.A. Atwater, J.J. Penninkhof, A. Polman, Physical Review B **71** (23): Art. No. 235408 JUN (2005).

19. **"The new "p-n junction". Plasmonics enables photonic access to the nanoworld"**, H.A. Atwater, S. Maier, A. Polman, J.A. Dionne, L. Sweatlock MRS Bulletin **30** (5): 385-389 May (2005)

20. **"Field-effect electroluminescence in silicon nanocrystals"**, R.J. Walters, G.I. Bourianoff, H.A. Atwater HA Nature Materials **4** (2): 143-146 FEB 2005

21. "**Quantum Efficiency of Silicon Nanocrystals in Dense Ensembles**", R. J. Walters, J. Kalkman, A. Polman, H. A. Atwater, and M. J. A. de Dood, Phys. Rev. Lett., submitted 2005.

22. **"Plasmon slot waveguides: Towards chip-scale propagation with subwavelength scale localization"**, J. A. Dionne, L. A. Sweatlock, Harry A. Atwater,A. Polman, Physical Review **B**, submitted 2005

23. "**Planar metal plasmon waveguides: frequency-dependent dispersion, propagation, localization, and loss beyond the free electron model**", J. A. Dionne, L. A. Sweatlock, and H. A. Atwater, A. Polman, Phys. Rev. B **72**, 075405 (2005).

24. "**Enhanced Radiative Emission Rate and Quantum Efficiency in Coupled Silicon Nanocrystal-Nanostructured Gold Emitters**", J.S. Biteen, D. Pacifici, N.S. Lewis, H.A. Atwater, Nano Lett.; **2005; 5** (9) pp 1768 – 1773

25. "**Optically triggered Q-switched photonic crystal laser**" Maune B, Witzens J, Jones TB, Kolodrubetz M, Atwater H, Scherer A, Hagen R, Qiu YM Optics Express **13** (12): 4699-4707 JUN 13 2005

a. **Invited Conference and Seminar Presentations**

Listed below is a summary of the 19 invited presentations given on the subject of plasmonic materials and devices under this contract during the period 4/1/03-3/31/04:

2005

7/23/05	Gordon Research Conference on Chemistry of Electronic Materials, New London, CT
7/13/05	International Conference on Quantum Electronics, Tokyo Japan
5/23/05	2nd International Conference on Surface Plasmon Photonics, Graz, Austria
5/10/05	Army Research Laboratory Workshop on Advanced Active Thin Films for Next Generation Meso/Microscale Army Applications, Destin, FL
4/14/05	SPIE Nanophotonics for Information Systems Conference, San Diego, CA
3/2505	Hewlett Packard Quantum Science Research 10th Anniversary Symposium, Palo Alto, CA
3/21/05	American Physical Society March Meeting, Los Angeles, CA
1/22/05	SPIE Photonics West, San Jose CA
1/21/05	DARPA Meeting on Photonics for Quantum Information Technology, Los Angeles, CA
1/5/05	Physics of Quantum Electronics Symposium, Snowbird UT

2004

12/13/04	Joop Los Fellowship Lecture, FOM Institute for Atomic and Molecular Physics, Amsterdam, the Netherlands
9/14/04	Annual Meeting, Stanford Photonics Research Center, Stanford CA
7/26/04	2nd International Nanophotonics Symposium, Osaka Japan
7/14/04	Laserion 2004, Castle Ringberg, Tegernsee Germany
5/20/2004	ONR Workshop on Epitaxial Engineering, Sorrell River Ranch, Utah
5//10/04	Nanophotonics Workshop, Defense Science Research Council, Washington DC
4/19/04	Distinguished Lecture Series, Department of Electrical Engineering, Iowa State University, Ames. IA
4/13/04	MRS Spring Meeting, Symposium L, San Francisco, CA
4/13/04	MRS Spring Meeting, Symposium R, San Francisco, CA
3/28/04	American Chemical Society 2004 Annual Meeting, Anaheim, CA
2/16/04	Workshop on Compound Semiconductor Materials and Devices, Pasadena, CA

2003

12/1/03	MRS Fall Meeting, Symposium V, Boston MA
11/1/03	Molecular Materials Symposium, Dartmouth College, Hanover, NH
10/13/03	Electrochemical Society Symposium, Orlando, FL
10/14/03	PIERS 2003, Honolulu, HI
9/12/03	IBM Almaden Research Center, San Jose, CA
8/8/03	Nanoscience Summer School, Argonne National Laboratory, Argonne, IL
6/27/03	Gordon Research Conference on Condensed Matter Physics, New London, CT
5/8/03	Materials Science Seminar, University of California, Berkeley, Berkeley CA
5/7/03	ONR Workshop on Heterogeneous Integration of Epitaxial Oxides, Fish Camp, CA
4/22/03	MRS Spring Meeting, Symposium A, San Francisco, CA
4/23/03	MRS Spring Meeting, Symposium H, San Francisco, CA
3/5/03	Optics and Quantum Electronics Seminar, MIT, Cambridge, MA
2/11/03	TinyTech Seminar, MIT, Cambridge, MA
1/22/03	DARPA Photonic Bandgap Crystal Workshop, San Diego, CA

2002

12/17/03	Components Research Seminar, Intel Portland Technology Division, Ronler Acres, OR
12/16/02	Nanoscience Seminar, Lawrence Livermore National Laboratory, Livermore, CA
11/27/02	MRS Fall Meeting, Symposium A, Boston MA
10/23/02	Condensed Matter Seminar, Harvard University, Cambridge, MA
10/6/02	International Workshop on Nanostructures for Electronics and Optics, Dresden, Germany
9/23/00	NATO Advanced Research Workshop, Trento Italy
8/3/02	FOM Institute for Atomic and Molecular Physics, Amsterdam, Netherlands

b. **Consultative and Advisory Functions**

1. Presenter and participant in Nanophotonics Workshop, Defense Science Research Council, Washington DC, 5/10/04
2. Presenter and participant in DARPA Meeting on Photonics for Quantum Information Technology, Los Angeles, CA, 1/21/05
3. I have acted as an informal consultant to DARPA program managers (S. Wolf, D. Healey, V. Browning and R. Athale) about the status of research in the plasmonics field.
4. Presentation to AFOSR Science Advisory Board during AFOSR program review, 7/19/05.
5. Founded Gordon Research Conference on Plasmonics, to be held first late July 2006.

c. **Transitions**. none

d. **New Discoveries, Inventions, or Patent Disclosures**.

"Optoelectronic Propagation and Switching Below the Diffraction Limit", Harry A. Atwater, Mark Brongersma and John Hartman, United State Patent Pending.

e. **Awards**

Joop Los Fellowship, awarded to Harry A. Atwater by Dutch FOM (Foundation on Fundamental Research on Matter.